electronic reprint

Journal of
Applied Crystallography
ISSN 0021-8898

Polycapillary optic–source combinations for protein crystallography

F. A. Hofmann, W. M. Gibson, C. A. MacDonald, D. A. Carter, J. X. Ho and J. R. Ruble

Journal of
Applied Crystallography
ISSN 0021-8898

Received 12 October 2000
Accepted 15 March 2001

Polycapillary optic–source combinations for protein crystallography

F. A. Hofmann,[a] W. M. Gibson,[a] C. A. MacDonald,[a]* D. A. Carter,[b] J. X. Ho[b] and J. R. Ruble[b]

[a]Center for X-Ray Optics, University at Albany, SUNY, Albany, NY 12222, USA, and [b]New Century Pharmaceuticals Inc., 895 Martin Rd, Huntsville, AL 35824, USA. Correspondence e-mail: c.macdonald@albany.edu

The work in this paper is a systematic study of the application of collimating and slightly focusing polycapillary optics to the X-ray crystallographic structure determination of egg-white lysozyme using two different sources: a standard rotating anode source and a low-power table-top microfocusing source. For the rotating anode source, a series of measurements comparing duplicate data sets obtained from the same individual crystal are summarized. Intensity and data quality are discussed for measurements with a pinhole collimator, a collimating polycapillary optic and a focusing polycapillary optic. The collected data were analyzed using conventional analysis software; limitations of the use of conventional analysis software for focused beams are discussed. Two data sets were collected using the low-power source and collimating optics, and three data sets using a lower-power source and focusing optics with three different limiting apertures.

1. Introduction

Polycapillary X-ray optics can be utilized to optimize the characteristics of X-ray beams for a variety of applications (Hofmann *et al.*, 1997, 1998; MacDonald, 1996; MacDonald *et al.*, 1999; MacDonald & Gibson, 2001). They collect X-rays over a wide solid angle from a divergent source and collimate them to a parallel beam using collimating optics, as shown in Fig. 1, or focus them to a convergent beam with focusing optics, as shown in Fig. 2, thus increasing the flux at the sample, while maintaining the necessary angular divergence and cross section. Different polycapillary optics configurations have been used successfully in the past for a variety of single-crystal diffraction applications, yielding gains of one to three orders of magnitude in direct-beam flux compared with conventional data collection methods using highly collimated beams created with pinhole collimators (Owens *et al.*, 1996).

2. Set up

A general schematic for the data collection with a collimating optic is shown in Fig. 1. The crystal holder, pinhole collimator and detector were first aligned with the X-ray source; then the optic was aligned to the beam axis. A nickel filter was used to minimize the Cu $K\beta$ radiation; no monochromator was employed. The schematic for a focusing optic is shown in Fig. 2.

2.1. Source and beam requirements

Before designing a polycapillary optic for macromolecular crystallography, one has to keep the source and beam requirements in mind. Typical requirements are a small, monochromatic and parallel beam. Most macromolecular crystals are between 0.3 mm and 0.5 mm in size. Pinhole collimators of the same size are used to minimize background. Usually the beam is then monochromated by diffracting the X-rays from *e.g.* the (002) planes of a graphite crystal. Also, a filter of an appropriate material is often placed in the beam (*e.g.* Ni foil for Cu-anode sources subtracts Cu $K\beta$ X-rays). The divergence of the beam at the crystal is usually determined by the size of the pinhole collimator and the distance of the source, and is usually less than 5 mrad, although the beam can be manipulated by X-ray mirrors, which may generate a focused beam with convergence of 10 mrad. Furthermore, there are source-specific requirements. Most macromolecular crystallographers use rotating anode X-ray sources with anode to window distances of 30 to 40 cm and standard spot sizes ranging from 0.1 × 1.0 mm to 0.5 × 10 mm. Some of these design specifications, such as the need for a rotating anode and a nearly parallel beam, prove to not be essential requirements for protein crystallography. However, we first take a look at polycapillary optics fabricated for such a rotating anode source and its application in a protein measurement.

2.2. Optic characterization

Two optics were manufactured taking the above requirements, particularly the minimum source to anode distance and need for a small beam at the crystal, into account. The rotating anode source used in this experiment has a modified shortened source to window distance of about 25 mm. The properties of the optics are described in Table 1. Figs. 2 and 3 show

Table 1
Properties of polycapillary optics fabricated for the rotating anode source.

The input and output 'diameters' are described in Fig. 3, while the length of the optic, L, the focal length, f, which is the distance from the source anode to the optic input, and the output focal length, F, which is the distance from the optic output to the focal spot at the crystal, are described in Fig. 2. The input capture angle, ω, is the input diameter divided by the input focal length, and is also shown in Fig. 2.

Property	Collimating optic	Slightly focusing optic
Output diameter D (mm)	4.02	3.56
Input diameter d (mm)	3.22	3.89
Length L (mm)	25	22
Input focus length f (mm)	35	50
Output focus length F (mm)	N/A	150
Input capture angle ω (rad)	0.09	0.08
Transmission (%)	~28	~20

the definitions of the various dimensions. The measured 'diameters' of the optic are actually flat-to-flat distances for the hexagonal cross section, as shown in Fig. 3. The optic transmission was measured for a small spot source at 8 keV.

3. Gain

If one talks about the gain of an optic, one has to specify the exact definition; there is direct-beam intensity gain, diffracted-beam intensity gain, signal-to-noise ratio, *etc*. This paper primarily discusses diffracted-beam intensity gain for complete data sets taken from a chicken egg-white lysozyme protein crystal. Special emphasis is placed on the discussion of the data quality, since a gain in diffracted-beam intensity with a corresponding loss in data quality is pointless. Similarly, a gain in direct-beam intensity cannot be translated into diffracted-beam intensity if part of the beam is not used.

To measure both the direct- and the diffracted-beam intensity gains, the optic was placed in an existing protein diffraction setup, consisting of a Rigaku RU-300 rotating anode X-ray source with a 0.3 × 3.0 mm source spot. The optic was mounted on micrometer-controlled stages, which allowed alignment in the X-ray beam, and positioned with the optic axis at an approximately 6–8° take-off angle. Direct-beam intensities were monitored with a Molecular Structure Corporation (MSC) PIN diode, which converts beam intensities into current. The direct beam operating at 40 kV and 60 mA (2.4 kW) through a 0.3 mm pinhole collimator yielded intensities from 0.9 to 1.0×10^{-4}. Before introduction of the optics, this system was used with a graphite monochromator for protein crystallography. Measured intensity after the monochromator was 5×10^{-6} (Owens *et al.*, 1996). Here, 1.0×10^{-4} is used as a standard for comparison in the remainder of the paper.

For the collimating optic, the direct-beam intensity through a 0.3 mm pinhole collimator is 4.2×10^{-4}, equivalent to an intensity gain of 4.2. For the slightly focusing optic, the direct-beam intensity through a 0.3 mm pinhole collimator is 2.0×10^{-3}, equivalent to an intensity gain of 20.

The diffracted-beam intensity was determined using the same protein crystal at the same orientation for both measurements, one with the optic and one without it. Setup-related restraints, including the time required to align the optic, made it necessary to acquire the data set with the optic before the data set without the optic. Since protein crystals undergo a continuous deterioration process after being exposed to ionizing radiation, the protein crystal often loses its diffraction ability before the end of the experiment. Besides keeping the crystal in a stream of cold nitrogen (the cryocooler shown in Figs. 1 and 2) to slow down the

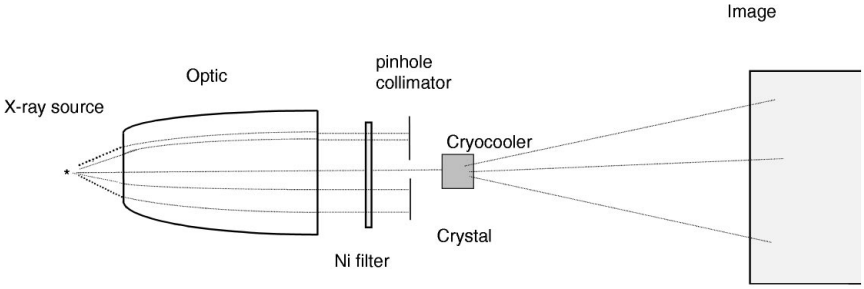

Figure 1
Schematic of setup including collimating optic.

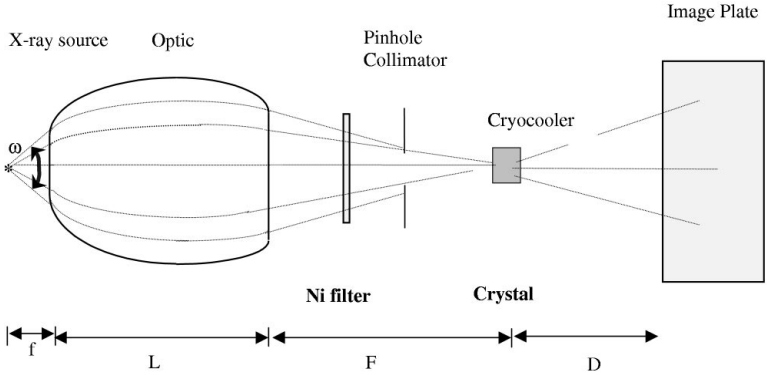

Figure 2
Schematic of setup including slightly focusing optic. The lengths f, L, F and D are given in Tables 1 and 5 for a variety of optics.

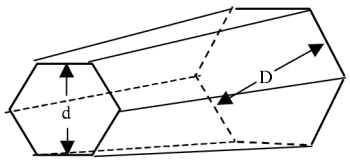

Figure 3
Schematic of input 'diameter' d and output 'diameter' D, specified in Tables 1 and 5.

deterioration process, it was necessary to monitor the degree of deterioration throughout the data acquisition process and reject bad data sets. Rejection of data sets usually occurred when the scale factor dropped below 90% of the original scale factor. Choosing only those diffraction spots for comparison that appeared in both data sets, the average intensity for the spots for each data set was determined. Figs. 4 and 5 show histograms of the ratios of intensities for reflections found in common. These histograms were obtained by dividing the intensity of each of the reflections acquired with the optic by the intensity of the corresponding reflection acquired without the optic, and then multiplying by the ratio of the exposure time per frame. Fitting these histograms with a Gaussian, a diffracted-beam intensity gain of 4.4 was recorded for the collimating optic and a diffracted beam intensity gain of 21.9 was recorded for the slightly focusing optic. These are consistent with the direct-beam intensity gains. Tables 2 and 3 show summaries of the results for both of these optics.

All the data were analyzed with conventional software. The applicability of the software could not be taken for granted since the diffraction spots will elongate in a highly convergent beam (Ho *et al.*, 1998) and start to overlap. Here, the convergence angle for the slightly focusing optic, calculated from the geometry of the setup, is about 0.3°. No decline in data quality was observed. One indication of the quality of the data is the crystallographic R factor describing the correctness of a model structure. The linear R factor (Drenth, 1994) is calculated from a set of observed structure factors $F_{\rm obs}$ and a set of calculated structure factors $F_{\rm calc}$,

$$R = \sum_{hkl} \big||F_{\rm obs}| - s|F_{\rm calc}|\big| \Big/ \sum_{hkl} |F_{\rm obs}|,$$

where s is a scale factor. These R factors for data sets collected with and without the optic are comparable and indicate the good quality of the measurements (6.9 and 6.4% for the protein crystal used for the comparison with and without the slightly focusing optic; 9.3 and 8.9% for the protein crystal used for the comparison with and without the collimating optic). The difference between the R factors for the collimating and focusing cases is caused by differences between the two crystals.

4. Low-power polycapillary-based system for protein crystallography

While the combination of rotating anode and polycapillary optic has been proven to be a powerful tool for macromolecular crystallography, there is ongoing work to develop a system that can offer the highest possible X-ray flux while being small, reliable, convenient and extremely affordable to use for laboratory-based rapid evaluation of crystal growth techniques, for determination of the purity and structural properties of protein crystals prior to eventual synchrotron-based high-resolution measurements, and for low-resolution analysis. A systematic study of the applications of polycapillary optics to the X-ray crystallographic structure determination of standard-system chicken egg-white lysozyme was performed, using a low-power (20 W) table-top microfocus

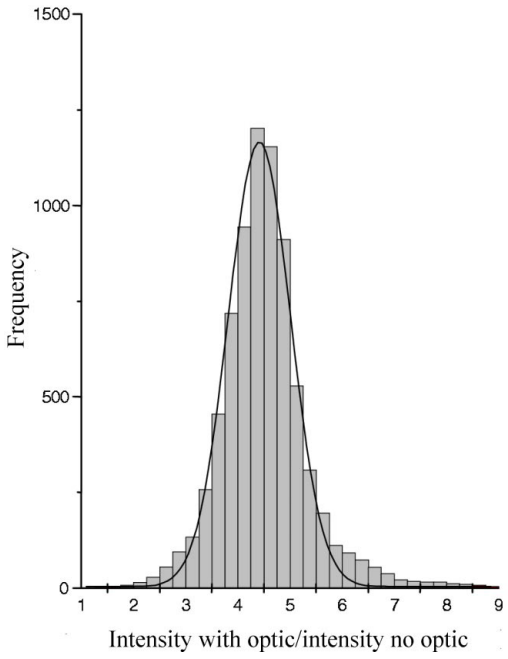

Figure 4
Histogram of the ratio of the intensity with the collimating optic to the intensity with no optic (see §3), for reflections identified to be in both data sets, obtained with the rotating anode source. Data were collected with the same individual protein crystal, with and without the optic.

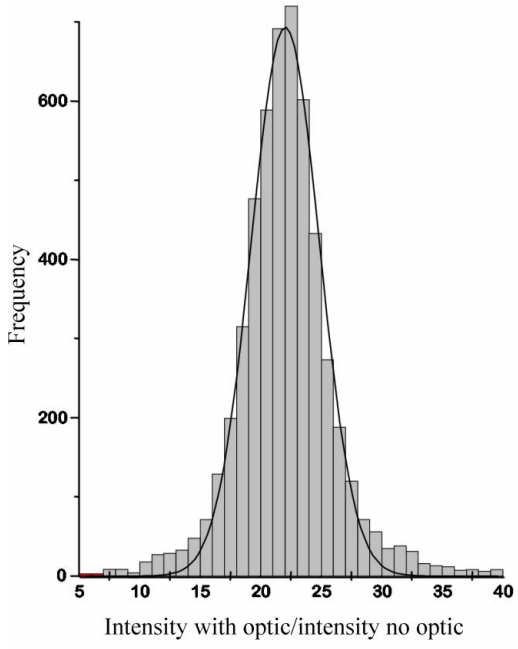

Figure 5
Histogram of the ratio of the intensity with the slightly focusing optic to the intensity with no optic (see §3), for reflections identified to be in both data sets, obtained with the rotating anode source. Data were collected with the same individual protein crystal, with and without the optic.

Table 2
Comparison of data with and without the collimating optic.

Both data sets were acquired on the same frozen chicken egg-white lysozyme crystal in 30 frames with an oscillation angle of 1.25° per frame. The source setting was 40 kV at 60 mA.

	With collimating optic	Without collimating optic
Optic	Collimating optic + 12.5 μm Ni	0.3 mm pinhole collimator + 12.5 μm Ni
Time per frame (min)	15	30
Average intensity of those reflections found in both sets	11676 ± 884	4141 ± 240
PIN diode intensity of direct beam	4.2×10^{-4}	1.0×10^{-4}
Linear *R* factor	0.093	0.089
Resolution (Å)	1.6	1.7

Table 3
Comparison of data with and without the slightly focusing optic.

Both data sets were acquired on a frozen chicken egg-white lysozyme crystal in 31 frames with an oscillation angle of 1.25° per frame. The source setting was 40 kV at 60 mA.

	With slightly focusing optic	Without slightly focusing optic
Optic	Slightly focusing optic + 0.3 mm pinhole collimator + 12.5 μm Ni	0.3 mm pinhole collimator + 12.5 μm Ni
Time per frame (min)	4	30
Average intensity of those reflections found in both sets	10082 ± 491	3911 ± 255
PIN diode intensity of direct beam	2.0×10^{-3}	1.0×10^{-4}
Linear *R* factor	0.069	0.064
Resolution (Å)	1.6 Å	1.6 Å

Table 4
Diffraction data for the combination of low-power source and collimating optic.

	Data set: collimating1	Data set: collimating2
Optic	Collimating optic + 600 μm pinhole collimator + 12.5 μm Ni	Collimating optic + 500 μm pinhole collimator + 12.5 μm Ni
Plate reader	Manual, with significant time variation between exposure and read	Automatic
Sample	Chicken egg-white lysozyme at room temperature	Chicken egg-white lysozyme at room temperature
Source setting	38 kV, 20 W	38 kV, 20 W
Oscillation angle (°)	2.0 (45 frames)	1.25 (72 frames)
Time per frame (min)	10	20
PIN diode intensity	1.0×10^{-4}	7.5×10^{-5}
Resolution (Å)	1.9	1.6
R factor (%)	11.6	5.1

X-ray source (Oxford X-ray Instruments) designed for optimum coupling with polycapillary collimating optics. The direct-beam intensity of data set 'collimating1' (Table 4), measured with an MSC PIN diode at 1.0×10^{-4}, is comparable with the direct-beam intensity obtained with the rotating anode source (Tables 2 and 3), despite the use of a source with a factor of 120 times lower power. The exposure time per frame with the low-power source was 10 min.

Table 5 lists the properties of the collimating and the focusing optic for the microfocus source. Notable are the short input focus lengths for the two optics, thus collecting X-rays from the source over a much wider acceptance angle. Table 4 shows the results for two complete data sets that have been acquired with this source–optic combination. Data set 'collimating1' was acquired with a combination of a manual image plate and scanner. The image plates had to be transported manually from the setup to the scanner, which introduced some time difference after exposure and before readout between the single frames. The time variation is believed to be responsible for the poor *R* factor. The time-variation problem was corrected for data set 'collimating2'. The image-plate detector transports the image plates automatically from the exposure to the readout to the erase position, which improves the accuracy of the intensity measurement. The *R* factor was determined as 5.1% and diffraction spots up to 1.6 Å resolution were detected with an exposure time of 20 min per frame. This measurement was performed with a 500 μm pinhole aperture, which explains the lower direct-beam intensity of 7.5×10^{-5}. The cryocooler used in the rotating anode system could not be incorporated in the measurement system, although that would be preferred in the future. Thus, comparison measurements could not be performed on the same crystal, because of crystal deterioration. In any case, it would not be possible to perform the comparison which was the most significant for the rotating anode source, the comparison between the optic and no optic case. For the low-power system, there is insufficient beam intensity to collect data without an optic.

Fig. 6 shows a diffraction image taken in 10 min with this source–collimating-optic combination.

Table 5
Properties of polycapillary optics fabricated for a microfocus source.

Property	Collimating optic for microfocus source	Slightly focusing optic for microfocus source
Output D (mm)	4.0	3.8
Input d (mm)	0.55	1.4
Length L (mm)	24.4	38
Input focus length (mm)	~3.8	8.5
Output focus length (mm)	N/A	105
Input capture angle ω (rad)	0.14	0.16
Transmission (%)	15 (Cu $K\alpha$)	20 (Cu $K\alpha$)

Table 6
Diffraction data for the combination of microfocus source and focusing optic.

	Data set: focusing1	Data set: focusing2	Data set: focusing3
Optic, filter	Focusing optic, 12.5 μm Ni foil	Focusing optic, 12.5 μm Ni foil	Focusing optic 610, 12.5 μm Ni foil
Aperture combination	1.5 mm entrance, 500 μm exit	2.0 mm entrance, 500 μm exit	3.0 mm entrance, 400 μm exit
Calculated convergence (°)	0.55	0.63	0.61
Measured convergence (°)	0.54	0.62	0.59
Source setting	38 kV, 20 W	38 kV, 20 W	38 kV, 20 W
Crystal	Chicken egg-white lysozyme	Chicken egg-white lysozyme	Chicken egg-white lysozyme
Frames	72 (20 min per frame)	72 (20 min per frame)	72 (20 min per frame)
Oscillation angle (°)	1.25	1.25	1.25
Direct beam intensity (MSC PIN diode)	5.0×10^{-5}	1.0×10^{-4}	9.0×10^{-5}
Apparent mosaicity (°)	0.741	0.83	0.915
Average intensity	4418	10159	5339
Linear R factor (%)	11.2	8.6	11.1
Total hkl	10462	12083	10688

Finally, data sets were taken with the microfocus source and a focusing optic that was manufactured to meet the necessary requirements of the source, the setup and the purpose of the measurements. The properties of the focusing optic are listed in Table 5; its output focus length is restricted by the minimum distance between source and crystal for the goniometer. A custom-made collimating aperture with adjustable length and exchangeable entrance and exit pinholes was necessary to control the convergence of the beam. In the experiment with the rotating anode source and slightly focusing optic, the convergence of the beam was small enough (0.3°) to be analyzed with conventional software, as mentioned above. For higher convergence angles, this is not necessarily possible. Here, the adjustable aperture allows an evaluation of a limiting convergence angle.

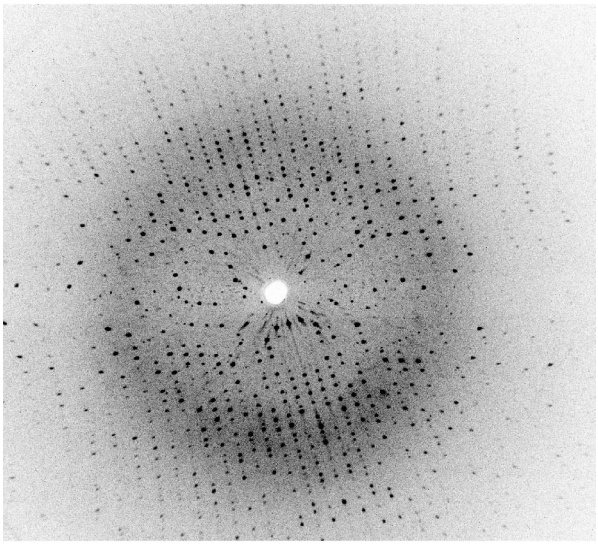

Figure 6
Lysozyme diffraction image taken with the combination of 20 W microfocus source and collimating polycapillary optic.

Three complete data sets with the same focusing optic and different pinhole aperture combinations were acquired for chicken egg-white lysozyme (Table 6). The measured convergence angle was the full width at half-maximum (FWHM) of a Gaussian fit to a measured Si-crystal rocking curve. The calculated convergence angle was from a simple Monte Carlo simulation, assuming a divergence from each channel of the optic of twice the critical angle. All the data sets could be analyzed with conventional software, but the quality of the analysis deteriorates with increasing convergence. The software tries to compensate for 'non parallel' X-rays by artificially increasing the apparent mosaicity of the crystal. The crystals used with the focusing optic show apparent mosaicities between 0.7° and 1.0°, whereas all the crystals used with a collimating optic or no optic have mosaicities between 0.25° and 0.45°, which is in agreement with reported mosaicities (Drenth, 1999). Also, as one can see in Fig. 7, the diffraction spots start to overlap for a convergence angle of about 0.6°. Especially as one moves to crystals with larger unit cells than lysozyme, the overlapping becomes a significant factor and one has a trade-off between the high flux produced by large convergence angles or the smaller diffraction spots produced by a smaller convergence (MacDonald *et al.*, 1999; Ho *et al.*, 1998). Development of analyzing software which can be used to process data from convergent beams becomes necessary and is underway (Ho *et al.*, 1998).

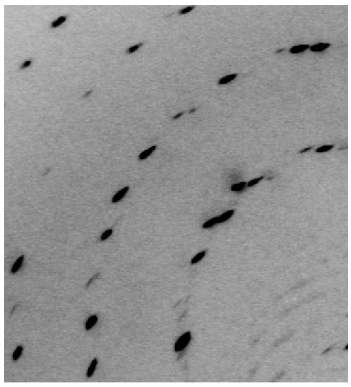

Figure 7
Lysozyme diffraction image taken with the combination of microfocus source and focusing optic, with 3.0 mm entrance aperture and 400 μm exit aperture (refer to data set 'focusing3' in Table 6).

Even with no convergence, *i.e.* the collimating lens, the largest resolvable unit-cell size is limited because of the local divergence, the divergence of X-rays from individual channels. For 8 keV X-rays, the local divergence was experimentally determined to be about 3 mrad (Owens, 1997). A diffracted spot separation with θ of 3 mrad corresponds to a unit-cell size of about 257 Å.

5. Conclusions

Performance and testing of polycapillary X-ray optics for macromolecular crystallography is advancing rapidly. In this work, the diffracted beam intensity gain was determined for a collimating optic and a slightly focusing optic on a rotating anode X-ray source. The results are consistent with the direct-beam intensity gain obtained previously. The collimating optic yields a gain of 4.4 and the slightly focusing optic yields a gain of 21.9 in diffracted beam intensity over the same system with no optic.

Furthermore, several useful data sets were successfully acquired with the combination of a low-power table-top X-ray source and polycapillary optic for both the collimating and the focusing optics. In this case, X-ray intensities comparable with those of a rotating anode source were obtained with 120 times lower X-ray power.

For convergent-beam protein crystallography, the use of conventional software for analyzing the data is possible but limited. Development of software for an X-ray beam with high convergence angle is underway (Ho *et al.*, 1998).

This work was supported by NASA under cooperative agreements NCC8-125 and NAS8-97247.

References

Drenth, J. (1994). *Principles of Protein X-ray Crystallography*, p. 285. New York: Springer.
Drenth, J. (1999). *Principles of Protein X-ray Crystallography*, 2nd edition, p. 104. New York: Springer.
Ho, J. X., Snell, E. H., Sisk, C. R., Ruble, J. R., Carter, D. C., Owens, S. M. & Gibson, W. M. (1998). *Acta Cryst.* D**54**, 200–214.
Hofmann, F. A., Freinberg-Trufas, C. A., Owens, S. M., Padiyar, S. D. & MacDonald, C. A. (1997). *Nucl. Instrum. Methods B*, **133**, 145–150.
Hofmann, F. A., Gibson, W. M., Lee, S. M. & MacDonald, C. A. (1998). *Polycapillary X-ray Optics for Thin Film Strain and Texture Analysis*, in *Thin Film Stresses and Mechanical Properties VII*, edited by R. C. Cammarata, M. A. Nastasi, E. P. Busso & W. C. Oliver, *Materials Research Society Proceedings*, Vol. 505.
MacDonald, C. A. (1996). *J. X-ray Sci. Technol.* **6**, 32–47.
MacDonald, C. A. & Gibson, W. M. (2001). *Polycapillary and Multichannel Plate X-ray Optics*, in *Handbook of Optics*, Vol. III, edited by M. Bass, ch. 30. New York: McGraw-Hill.
MacDonald, C. A., Owens, S. M. & Gibson, W. M. (1999). *J. Appl. Cryst.* **32**, 160–167.
Owens, S. M. (1997). PhD dissertation, Physics Department, University at Albany, SUNY.
Owens, S. M., Ullrich, J. B., Ponomarev, I. Yu., Carter, D. C., Sisk, C. R., Ho, J. X. & Gibson, W. M. (1996). *SPIE Proc.* **2859**, 200–209.